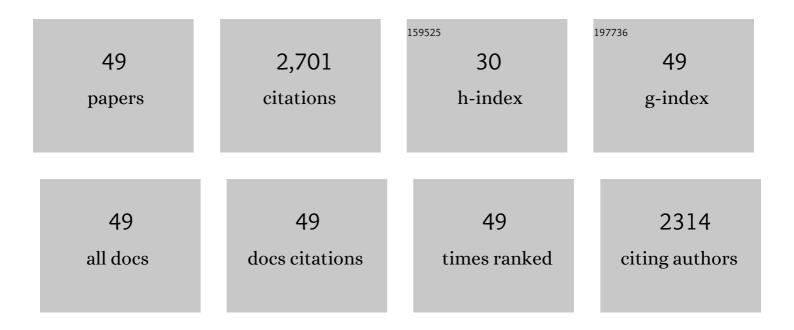
Min Wang

List of Publications by Year in descending order

Source: https://exaly.com/author-pdf/4533788/publications.pdf Version: 2024-02-01



MIN MANC

#	Article	IF	CITATIONS
1	N-doped graphitic carbon-incorporated g-C3N4 for remarkably enhanced photocatalytic H2 evolution under visible light. Carbon, 2016, 99, 111-117.	5.4	343
2	Two dimensional Co3O4/g-C3N4 Z-scheme heterojunction: Mechanism insight into enhanced peroxymonosulfate-mediated visible light photocatalytic performance. Chemical Engineering Journal, 2020, 398, 125569.	6.6	138
3	Characterization and photocatalytic properties of N-doped BiVO4 synthesized via a sol–gel method. Journal of Alloys and Compounds, 2013, 548, 70-76.	2.8	133
4	Synthesis of hollow lantern-like Eu(III)-doped g-C3N4 with enhanced visible light photocatalytic perfomance for organic degradation. Journal of Hazardous Materials, 2018, 349, 224-233.	6.5	120
5	Dual Z-scheme MoS2/g-C3N4/Bi24O31Cl10 ternary heterojunction photocatalysts for enhanced visible-light photodegradation of antibiotic. Journal of Alloys and Compounds, 2020, 825, 153975.	2.8	111
6	Effective visible light-active boron and europium co-doped BiVO4 synthesized by sol–gel method for photodegradion of methyl orange. Journal of Hazardous Materials, 2013, 262, 447-455.	6.5	110
7	Enhanced visible light photocatalytic degradation of tetracycline by MoS2/Ag/g-C3N4 Z-scheme composites with peroxymonosulfate. Applied Surface Science, 2020, 514, 146076.	3.1	106
8	Synthesis of novel Co3O4 hierarchical porous nanosheets via corn stem and MOF-Co templates for efficient oxytetracycline degradation by peroxymonosulfate activation. Chemical Engineering Journal, 2020, 392, 123789.	6.6	97
9	CuO/g-C3N4 2D/2D heterojunction photocatalysts as efficient peroxymonosulfate activators under visible light for oxytetracycline degradation: Characterization, efficiency and mechanism. Chemical Engineering Journal, 2021, 416, 128118.	6.6	95
10	The enhanced peroxymonosulfate-assisted photocatalytic degradation of tetracycline under visible light by g-C3N4/Na-BiVO4 heterojunction catalyst and its mechanism. Journal of Environmental Chemical Engineering, 2021, 9, 105524.	3.3	88
11	NiO/g-C3N4 2D/2D heterojunction catalyst as efficient peroxymonosulfate activators toward tetracycline degradation: Characterization, performance and mechanism. Journal of Alloys and Compounds, 2021, 880, 160547.	2.8	82
12	Effects of Cu dopants on the structures and photocatalytic performance of cocoon-like Cu-BiVO4 prepared via ethylene glycol solvothermal method. Journal of Alloys and Compounds, 2017, 691, 8-14.	2.8	73
13	The effects of bismuth (III) doping and ultrathin nanosheets construction on the photocatalytic performance of graphitic carbon nitride for antibiotic degradation. Journal of Colloid and Interface Science, 2019, 533, 513-525.	5.0	72
14	Novel rugby-like g-C3N4/BiVO4 core/shell Z-scheme composites prepared via low-temperature hydrothermal method for enhanced photocatalytic performance. Separation and Purification Technology, 2020, 232, 115937.	3.9	65
15	Thiourea-assisted one-step fabrication of a novel nitrogen and sulfur co-doped biochar from nanocellulose as metal-free catalyst for efficient activation of peroxymonosulfate. Journal of Hazardous Materials, 2021, 416, 125796.	6.5	64
16	Fabrication of novel ternary heterojunctions of Pd/g-C3N4/Bi2MoO6 hollow microspheres for enhanced visible-light photocatalytic performance toward organic pollutant degradation. Separation and Purification Technology, 2019, 211, 1-9.	3.9	63
17	Catalytic degradation of oxytetracycline via FeVO4 nanorods activating PMS and the insights into the performance and mechanism. Journal of Environmental Chemical Engineering, 2021, 9, 105864.	3.3	60
18	Hydrothermal synthesis of Sm-doped Bi2MoO6 and its high photocatalytic performance for the degradation of Rhodamine B. Journal of Alloys and Compounds, 2017, 728, 739-746.	2.8	58

Min Wang

#	Article	IF	CITATIONS
19	Electro-assisted heterogeneous activation of peroxymonosulfate by g-C3N4 under visible light irradiation for tetracycline degradation and its mechanism. Chemical Engineering Journal, 2022, 436, 135278.	6.6	54
20	The construction of g-C3N4/Sm2+ doped Bi2WO6 2D/2D Z-scheme heterojunction for improved visible-light excited photocatalytic efficiency. Separation and Purification Technology, 2019, 224, 33-43.	3.9	53
21	Eu doped g-C3N4 nanosheet coated on flower-like BiVO4 powders with enhanced visible light photocatalytic for tetracycline degradation. Applied Surface Science, 2018, 453, 11-22.	3.1	52
22	High performance B doped BiVO4 photocatalyst with visible light response by citric acid complex method. Spectrochimica Acta - Part A: Molecular and Biomolecular Spectroscopy, 2013, 114, 74-79.	2.0	51
23	Effective visible light-active nitrogen and samarium co-doped BiVO4 for the degradation of organic pollutants. Journal of Alloys and Compounds, 2015, 648, 1109-1115.	2.8	45
24	Ag, B, and Eu tri-modified BiVO4 photocatalysts with enhanced photocatalytic performance under visible-light irradiation. Journal of Alloys and Compounds, 2018, 753, 465-474.	2.8	45
25	The enhanced photocatalytic activity of Ag-OVs-(0Â0Â1) BiOCl by separating secondary excitons under double SPR effects. Applied Surface Science, 2020, 526, 146689.	3.1	44
26	The enhanced P-nitrophenol degradation with Fe/Co3O4 mesoporous nanosheets via peroxymonosulfate activation and its mechanism insight. Journal of Alloys and Compounds, 2021, 858, 157739.	2.8	41
27	Hydrothermal synthesis of B-doped Bi2MoO6 and its high photocatalytic performance for the degradation of Rhodamine B. Journal of Physics and Chemistry of Solids, 2018, 113, 86-93.	1.9	38
28	Enhanced visible-light-driven photocatalytic activity of B-doped BiVO4 synthesized using a corn stem template. Materials Science in Semiconductor Processing, 2015, 30, 307-313.	1.9	33
29	The promoted tetracycline visible-light-driven photocatalytic degradation efficiency of g-C3N4/FeWO4 Z-scheme heterojunction with peroxymonosulfate assisting and mechanism. Separation and Purification Technology, 2022, 296, 121440.	3.9	32
30	Novel binary of g-C 3 N 4 coupling and Eu 3+ doping co-modifying bidirectional dendritic BiVO 4 heterojunctions with enhanced visible-light photocatalytic performance. Separation and Purification Technology, 2018, 202, 335-344.	3.9	30
31	A facile synthesis of nano-layer structured g-C3N4 with efficient organic degradation and hydrogen evolution using a MDN energetic material as the starting precursor. International Journal of Hydrogen Energy, 2019, 44, 4102-4113.	3.8	30
32	Eu2O3/Co3O4 nanosheets for levofloxacin removal via peroxymonosulfate activation: Performance, mechanism and degradation pathway. Separation and Purification Technology, 2021, 274, 118666.	3.9	27
33	Peroxymonosulfate activation by cobalt particles embedded into biochar for levofloxacin degradation: Efficiency, stability, and mechanism. Separation and Purification Technology, 2022, 294, 121082.	3.9	26
34	The effect of pH on the photocatalytic performance of BiVO4 for phenol mine sewage degradation under visible light. Optik, 2019, 179, 672-679.	1.4	25
35	Enhanced Mediated Electron Transfer Pathway of Peroxymonosulfate Activation Dominated with Graphitic-N for the Efficient Degradation of Various Organic Contaminants in Multiple Solutions. ACS ES&T Water, 2022, 2, 817-829.	2.3	25
36	Effects of Ni doping contents on photocatalytic activity of B-BiVO 4 synthesized through sol-gel and impregnation two-step method. Transactions of Nonferrous Metals Society of China, 2017, 27, 2022-2030.	1.7	19

Min Wang

#	Article	IF	CITATIONS
37	Bi3.64Mo0.36O6.55/Bi2MoO6 heterostructure composite with enhanced photocatalytic activity for organic pollutants degradation. Journal of Alloys and Compounds, 2018, 766, 1037-1045.	2.8	19
38	The facile fabrication of g-C3N4 ultrathin nanosheets with higher specific surface areas for highly sensitive detection of trace cadmium. Measurement: Journal of the International Measurement Confederation, 2019, 140, 548-556.	2.5	19
39	Electro-enhanced sulfamethoxazole degradation efficiency via carbon embedding iron growing on nickel foam cathode activating peroxymonosulfate: Mechanism and degradation pathway. Journal of Colloid and Interface Science, 2022, 624, 24-39.	5.0	19
40	The honeycomb-like Eu3+, Fe3+ doping bismuth molybdate photocatalyst with enhanced performance prepared by a citric acid complex process. Materials Letters, 2017, 192, 96-100.	1.3	17
41	0D/1D BiVO4/CdS Z-scheme nanoarchitecture for efficient photocatalytic environmental remediation. Colloids and Surfaces A: Physicochemical and Engineering Aspects, 2022, 650, 129583.	2.3	14
42	Highly sensitive detection of trace Hg2+ via PdNPs/g-C3N4 nanosheet-modified electrodes using DPV. Microchemical Journal, 2020, 152, 104356.	2.3	12
43	The research of lead ion detection based on rGO/g-C3N4 modified glassy carbon electrode. Microchemical Journal, 2020, 157, 105076.	2.3	11
44	MoS2 and g-C3N4 nanosheet co-modified Bi2WO6 ternary heterostructure catalysts coupling with H2O2 for improved visible photocatalytic activity. Materials Chemistry and Physics, 2021, 272, 124982.	2.0	11
45	Construction of g-C3N4/Eu(III) doped Bi24O31Cl10 heterojunction for the enhanced visible-light photocatalytic performance. Materials Chemistry and Physics, 2019, 237, 121829.	2.0	8
46	Solution combusting synthesis of xFe-Bi2MoO6 nanoparticles with increased photocatalytic performance for organic pollutants degradation. Optik, 2020, 222, 165399.	1.4	8
47	Effect of calcination temperature on the structure and photocatalytic performance of BiVO ₄ prepared via an improved solution combustion method. Micro and Nano Letters, 2018, 13, 1017-1020.	0.6	7
48	Stable LSPR effect and full-spectrum photocatalytic water purification by g-C3N4â^'x/MoO3â^'x with passivated interface oxygen vacancies. Journal of Alloys and Compounds, 2022, 891, 161928.	2.8	7
49	Fabrication of Co3+ and B co-doping BiVO4 with improved photocatalytic performance for organic degradation. MATEC Web of Conferences, 2018, 238, 03008.	0.1	1